Computers and Geotechnics xxx (2009) xxx–xxx

Contents lists available at ScienceDirect

Computers and Geotechnics

journal homepage: www.elsevier.com/locate/compgeo

# Coupling between finite and discrete element methods for the modelling of earth structures reinforced by geosynthetic

P. Villard, B. Chevalier *, B. Le Hello, G. Combe

*Grenoble Universités, Laboratoire Sols, Solides, Structures – Risques, UMR CNRS/UJF/INPG, Domaine Universitaire BP 53, 38 041 Grenoble Cedex 9, France*

ARTICLE INFO

*Article history:*
Received 9 July 2008
Received in revised form 24 October 2008
Accepted 28 November 2008
Available online xxxx

*Keywords:*
Numerical model
Discrete element method
Finite element method
Coupling
Reinforced soils
Sinkhole
Geosynthetics

ABSTRACT

Due to the use of new technologies and innovative materials in civil engineering (reinforcement, recycled or natural materials), the design of geotechnical earth structures has become more complex, involving improvements to existing numerical models in order to consider the specific mechanical behaviours of each component in the structure. In this article, we focus on a new numerical model dedicated to earth structures reinforced with geosynthetic sheets, based on coupling the finite element method (FEM) and the discrete element method (DEM). The numerical model proposed takes the tensile and membrane behaviours of the geosynthetic into account by the FEM, and the interface friction between soil and geosynthetic and granular soil behaviour under large displacements by the DEM. The model used to describe the membrane and the tensile behaviours of the geosynthetic sheet is presented, and the basic assumptions of the discrete element method are then set out. Particular attention was paid to the description of the geometrical and micro-mechanical parameters of the discrete particle assemblies needed to reproduce realistic behaviour of granular soils. The aim of this article is to model the interaction between the geosynthetic sheet and the particles of soil, so the numerical coupling of FEM–DEM is described in detail; in particular, a specific contact law relating to the friction behaviour of the composite soil–geosynthetic is proposed. To show the interest of the numerical developments in modelling reinforced earth structures, an application is provided for embankments, reinforced at their base by a geosynthetic and built on areas subject to potential sinkholes. The numerical results of the FEM–DEM coupling are compared to those of true-scale instrumented experiments and of an analytical design method. The qualitative and quantitative comparisons of strains and tensile forces acting on the geosynthetic sheet make it possible to validate the numerical model suggested.



## 1. Introduction

In many countries, the development of new road and railway infrastructures requires the use of geological areas characterized by weak or heterogeneous mechanical properties, for economic and technical reasons. In such cases, reinforcement techniques (piles, geosynthetics, nails, etc.) are to be implemented to ensure the stability and longevity of the structures. Due to the use of several components with different rigidity and to the complexity of interaction mechanisms, designing these composite structures has become increasingly difficult. The use of a numerical model is therefore necessary to take into account the behaviour of each component in the structure and the interaction between them.

Among the usual techniques used, the reinforcement of earth structures by geosynthetic sheets is currently widespread because it saves time and has a moderate cost. In order to improve the behaviour of this kind of structure, we propose a new numerical approach for the modelling of geosynthetic-reinforced earth structures which can take the behaviour of each material (granular soil and geosynthetic sheet) and their interaction into account accurately. A mixed method was proposed based on coupling the finite and discrete element methods. Application to the reinforcement of rail and road bedding layers, by underlying geosynthetic sheets in areas prone to local subsidence, was performed in order to illustrate the interest of the numerical model proposed. Where the ground was subsiding, a geosynthetic reinforcement layer was placed at the base of road and rail embankments. The aim of this reinforcement was to alert operators that a sinkhole was beginning to form and to limit surface subsidence to permissible values so as to allow traffic circulation and the safety of users until backfilling and repair works on the fill material could be implemented.

When sinkholes appear, these structures are subject to large deformations that induce a change in the orientation of forces within the granular material (arching effect or transfer of load). So only part of the force (tensile stress) applied to the structure is transferred to the geosynthetic sheet placed over the cavity.

* Corresponding author. Tel.: +33 04 56 52 86 28; fax: +33 04 76 82 70 43.
*E-mail addresses:* pascal.villard@ujf-grenoble.fr (P. Villard), bastien.chevalier@ujf-grenoble.fr (B. Chevalier).

0266-352X/$ - see front matter © 2008 Elsevier Ltd. All rights reserved.
doi:10.1016/j.compgeo.2008.11.005

**Nomenclature**

| | |
|---|---|
| $C_e$ | expansion coefficient of granular soil embankment (–) |
| $D$ | diameter of soil particles (m) |
| $E_0$ | macroscopic tangential stiffness modulus at the interface (N/m3) |
| $E$ | microscopic tangential stiffness modulus at the interface (N/m$^3$) |
| $e$ | thickness of the geosynthetic sheet (m) |
| $f$ | maximum vertical displacement of the geosynthetic sheet (m) |
| $F$ | forces acting on the nodes of a triangular finite element (N) |
| $F_u$ | corrective vector force coefficients of a triangular finite element (N/m) |
| $H$ | granular soil embankment thickness (m) |
| $J$ | geosynthetic stiffness (N/m) |
| $k_n$ | normal stiffness of discrete element contact (N/m) |
| $k_{ni}$ | normal interface stiffness between finite and discrete elements (N/m) |
| $k_t$ | shear stiffness of discrete element contact (N/m) |
| $k_{ti}$ | shear interface stiffness between finite and discrete element (N/m) |
| $K_u$ | coefficients of the elementary matrix of rigidity of a triangular finite element (N/m) |
| $L$ | cavity width (m) |
| $L_{Gl}$ | length of the sheet from the left end to the middle of the cavity (m) |
| $L_{Gd}$ | length of the sheet from the right end to the middle of the cavity (m) |
| $P_r$ | relative porosity (–) |
| $q$ | vertical load acting over the cavity (N/m) |
| $q_0$ | vertical load acting on anchorage areas (N/m$^2$) |
| $t$ | time step of the centred finite difference algorithm (s) |
| $S$ | influence area of the contact (m$^2$) |
| $T$ | tension in the geosynthetic sheet (N/m) |
| $T_{max}$ | maximal tensile force acting on the geosynthetic sheet (N/m) |
| $u$ | nodal displacements of a triangular finite element (m) |
| $U_0$ | relative displacement from which the friction mobilization becomes maximum (m) |
| $U_n$ | normal overlap between finite and discrete elements (m) |
| $U_t$ | tangential overlap between finite and discrete elements (m) |
| $V$ | volume of a sample of soil under triaxial test (m$^3$) |
| $\delta$ | interface friction angle (°) |
| $\delta_{lower}$ | lower interface friction angle between subsoil and geosynthetic (°) |
| $\delta_{upper}$ | upper interface friction angle between granular soil and geosynthetic (°) |
| $\varepsilon$ | sheet strain of the geosynthetic sheet (–) |
| $\varepsilon_1$ | axial strain of a sample of soil under triaxial test (–) |
| $\phi$ | internal friction angle of granular fill soil (°) |
| $\gamma$ | unit weight of granular fill soil (N/m$^3$) |
| $\eta$ | initial porosity of particles soil assembly (–) |
| $\eta_{max}$ | maximal porosity of particles soil assembly (–) |
| $\eta_{min}$ | minimal porosity of particles soil assembly (–) |
| $\mu$ | microscopic friction angle of discrete element contact (°) |
| $\sigma$ | tensile stress supported by a set of fibres o the geosynthetic sheet (N/m$^2$) |
| $\sigma_1$ | compressive pressure of a sample of soil under triaxial test (N/m$^2$) |
| $\sigma_3$ | confine pressure of a sample of soil under triaxial test (N/m$^2$) |
| $\sigma_n$ | normal stress applied on the interface (N/m$^2$) |
| $\tau$ | friction stress at the interface between soil and geosynthetic (N/m$^2$) |
| $\tau_{max}$ | maximum friction stress at the interface between soil and geosynthetic (N/m$^2$) |

On both sides of the cavity the tensile forces acting on the geosynthetic are balanced by frictional forces.

Not all these complex mechanisms are taken into account correctly in the design analytical methods currently used in engineering. Surface settlement and the stresses acting on the geosynthetic are not properly evaluated.

The originality of the numerical model presented in this article consists in a coupling between the finite element model used for the geosynthetic sheet and the discrete element methods used to describe the behaviour of granular soil. The finite element model describes the fibrous structure and the directions of reinforcement of the geosynthetic sheet by means of a specific matrix of rigidity. The membrane and tensile behaviour of the sheet can easily be restored (no bending or compression in fibres). The granular soil is modelled by a set of particles which can move more or less easily depending on the type of stress applied. This method allows naturally large displacement and makes it possible to take into account complex mechanisms such as rolling, expansion, transfer of load, arching effect and collapses. Special attention is paid to the interactions by friction between the FEM and the DEM by means of specific contact laws.

## 2. The numerical model

The numerical approach chosen to allow the coupling between the discrete and finite element methods consists in including the specific finite elements characteristic of the geosynthetic sheet in a 3D discrete element code (S.D.E.C. for spherical discrete element code) [13,14]. The behaviour of the finite elements is governed, in the same way as the discrete elements, by Newton's law of motion. The interaction between the two kinds of elements is defined by specific contact laws at each contact point.

### 2.1. The finite element model

The finite elements used to model the behaviour of the geosynthetic sheet are triple-node triangular elements [28] taking into account the fibrous structure of the geosynthetic (knitted, woven or non-woven geosynthetic, reinforced or not in particular directions) through the fibre orientation distribution density. These elements allow us to describe the tensile and membrane behaviour of the sheet under large deformation (due to their constitution, geosynthetic sheets have no bending and no compressive rigidities). The numerical model was validated by comparison with analytical solutions of the membrane effect obtained in simple cases [28] and with experimental results of laboratory tests or full-scale experiments [29,21].

The fundamental assumptions made to establish the behaviour of a three-node element are:

- Each element consists of a set of fibres with various orientations, initially forming a plan,

Please cite this article in press as: Villard P et al., Coupling between finite and discrete element methods for the modelling ..., Comput Geotech (2009), doi:10.1016/j.compgeo.2008.11.005

- There is no slipping between the fibres (presence of connection points between wires). Consequently the behaviour of a fibre network is obtained by superposition of behaviours obtained in each fibre direction.
- The tensile forces acting in each fibre are oriented in the direction of this fibre after deformation (large displacements).
- The mechanical behaviour of the fibre is non-linear elastic.
- The compression elastic modulus is very weak compared with the tensile elastic modulus (no compression in fibres).
- There are no bending stresses.

For each three-node element, an elementary relation between the nodal displacements and the external forces applied to the element can be written:

$$\{\vec{F}\} = [K_u]\{\vec{u}\} + \{\vec{F}_u\} \quad (1)$$

$\{\vec{F}\}$ are the forces acting on the nodes of an element, $\{\vec{u}\}$ the nodal displacements of the element, $(K_u)$ the elementary matrix of rigidity depending on the final position of the three nodes, and $\{\vec{F}_u\}$ a corrective vector force resulting from the large displacement formulation. This basic relation [28,29], characteristic of the mechanical behaviour of a triangular finite element, is used in the iterative process of calculation included in the coupling code.

### 2.2. The discrete element model

The discrete element model used is based on the molecular dynamics approach first developed by Cundall and Strack [11]. The DEM assumes a set of particles interacting at contact points, making it possible to describe the behaviour of granular soils under large deformations (shear banding, crushing or overall rotation). The discrete element software used for this study is a three-dimensional code [13] using spherical particles which can be joined together to make clusters of various shapes. The general algorithm of calculation used consists in successively alternating the application of Newton's second law of motion to the particles and force–displacement laws to the contacts. The motion equations are integrated using an explicit centred finite difference algorithm involving a time step $\Delta t$.

Interaction laws, defined for a local scale, make it possible to reproduce the global macroscopic behaviour of the particle assembly. Elastic behaviour depends on two local contact parameters: normal stiffness $k_n$ and shear stiffness $k_t$. For granular materials, a frictional contact failure criterion based on the elastic perfectly plastic model proposed by Cundall and Strack [11] is defined using a microscopic friction angle $\mu$.

The set of micro-mechanical parameters ($k_n$, $k_{tn}$ and $\mu$) and geometrical parameters (particle size distribution, particle shapes and porosity of the assembly) influences the macro-mechanical properties of the granular matter. For numerical modelling of true-scale structures, the aim is not to reproduce the real grain morphology, particle size distribution or particle number, as this would imply a prohibitive calculation period. However, for a simplified geometry (particle shape and particle size distribution), we focused on the determination of micro-mechanical parameters giving macro-mechanical characteristics analogous to real geomaterials like soils (in dense or loose states).

In order to build numerical particle assemblies with different porosity, the particles were set up using the radius expansion with decrease of friction process (REDF) [10]. This methodology allows homogeneous and isotropic particle assemblies to be built.

The function that connects the micro-mechanical and physical parameters to the macro-mechanical characteristics of assemblies is very complex and for the most part undetermined, mainly because of the multiple parameters involved. Generally, clumps of spheres (referred to as "clusters") are preferred to single spheres in order to obtain realistic behaviour of the granular materials (due to an excessive rolling between the particles, spherical particles assemblies lead to lower global failure parameters).

Numerical simulations of triaxial tests performed by means of "clusters" made of three or four particles have shown the ability of Discrete Element Modelling to reproduce the behaviour of geomaterials reliably [24]. For example, for a given particle shape and a given set of micro-mechanical parameters, it is possible to describe the influence of the density of an assembly on the response to a triaxial test, like for actual geomaterials [24].

In the case of the present study, the micro-mechanical parameters were set in order to obtain shear strengths of the numerical assembly (quantified by the peak and residual friction angles) similar to those of the actual material. The shear strength of the numerical assemblies was defined as the response of fictional triaxial tests made on the elementary representative volume of particles. In order to show the analogy between the response of a numerical particle assembly and a real geomaterial, numerical triaxial tests were performed with a set of micro-mechanical parameters ($k_n$, $k_t$ and $\mu$), for several porosities and a constant confining pressure of 10 kPa:

- The minimal porosity ($\eta_{\min} = 0.305$) was obtained using the REDF process by taking a microscopic friction angle equal to zero during the radius expansion phase.
- The maximal porosity ($\eta_{\max} = 0.420$) was obtained in the same way, using a fixed microscopic friction angle equal to $\mu$.
- Two relative porosities $P_r$ defined by Eq. (2) were also considered: $P_r = 87\%$ ($\eta = 0.320$) and $P_r = 35\%$ ($\eta = 0.380$).

The numerical samples were made up of 8000 clusters of two overlapped spheres of diameter $D$. The maximal length of a cluster was 1.5 $D$, with $D$ ranging randomly between two extreme values defined by a ratio of 1.333.

$$P_r = (\eta_{max} - \eta)/(\eta_{max} - \eta_{min}) \quad (2)$$

The numerical results of the triaxial tests are given in Figs. 1 and 2 (deviatoric stress and volumetric stain versus axial strain). In these figures we note the ability of the discrete element model to describe the mechanical behaviour of granular materials (critical state, dilatancy, influence of porosity) very satisfactorily. For the granular material modelled, the maximal macroscopic friction angle obtained at the peak was 44.8°.

### 2.3. Interaction between finite and discrete elements

Specific interaction laws are used to describe the interface behaviour between the soil particles and the triangular finite ele-

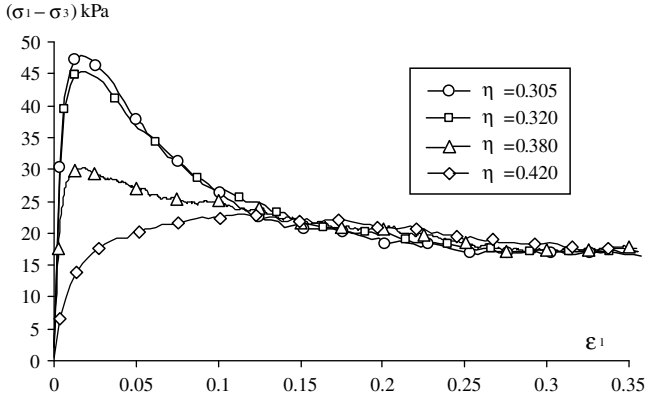


**Fig. 1.** Numerical results of triaxial tests: deviator stress versus axial strain.

Please cite this article in press as: Villard P et al., Coupling between finite and discrete element methods for the modelling ..., Comput Geotech (2009), doi:10.1016/j.compgeo.2008.11.005

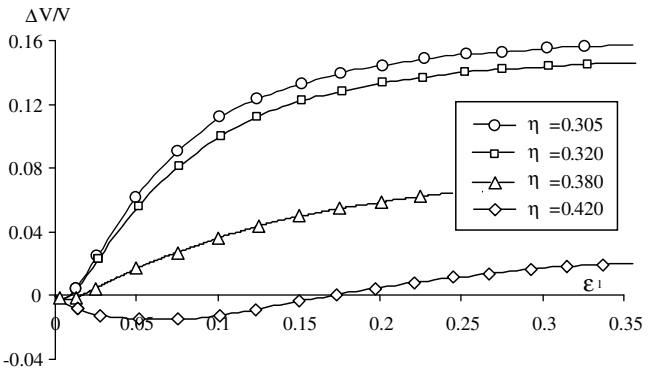


**Fig. 2.** Numerical results of triaxial tests: volumetric strains versus axial strain.

ments. The contact parameters are the normal contact stiffness $k_{ni}$ necessary to guarantee no major interpenetration between the finite and discrete elements, tangential contact stiffness $k_{ti}$ and the interface friction angle $\delta$ to define the failure criterion. The normal contact force $\{\vec{F}_n\}$ between the finite and discrete elements can be written by Eq. (3) where $\{\vec{U}_n\}$ is the overlap between two elements:

$$\{\vec{F}_n\} = k_{ni}\{\vec{U}_n\} \tag{3}$$

We note that the behaviour in friction is independent from the value of the normal stiffness $k_{ni}$ of the contact between the soil and geosynthetic sheet elements. A large value for $k_{ni}$ is considered in order to guarantee a reduced overlap between the soil and geosynthetic sheet elements.

The tangential contact forces $\vec{F}_t$ applied to the finite and discrete elements are linked to the tangential incremental relative displacement $\vec{U}_t$ by the expression:

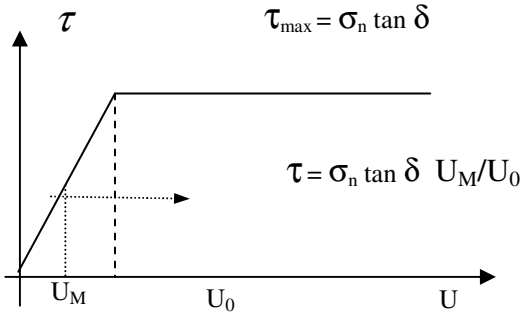


**Fig. 3.** Friction interface criterion.

$$\mathrm{d}(\vec{F}_t)/\mathrm{d}(\vec{U}_t) = k_{ti} \quad \text{with } |\vec{F}_t| \leqslant |\vec{F}_n| tg(\delta) \tag{4}$$

The macroscopic behaviour of contact between soil particles and geosynthetic sheets is characterized through experimental laboratory tests (frictional or pull-out tests). A simple law of friction (Fig. 3) is deduced from these tests connecting the tangential stress $\tau$ at the interface to the relative displacement $U$ between soil particles and the geosynthetic sheet. $U_0$ represents the relative displacement necessary to mobilize the friction fully and $E_0$ the tangential stiffness modulus at the interface (in N/m$^3$) defined by Eq. (5). $\sigma_n$ is the normal stress acting at the interface.

$$E_0 = \tau_{\max}/U_0 \tag{5}$$

with:

$$\tau_{\max} = \sigma_n \tan\delta \tag{6}$$

$U_0$ depends on the characteristics of the soil/sheet interaction, on the roughness of the elements in contact, on the rolling of soil particles and on the value of normal stress $\sigma_n$. $U_0$ does not usually exceed a few millimetres. $\delta$ is the macroscopic angle of friction between the soil and geosynthetic sheet as defined in the numerical model.

$K_{ti}$ (in N/m) is a microscopic parameter of the tangential contact between a particle of soil with no rolling and a sheet element supposed to be fixed (no extension possible). With these assumptions, $K_{ti}$ cannot be directly linked to the macroscopic stiffness modulus $E_0$ obtained from experimental friction tests: the rolling of soil particles and the stretching of the sheet element cannot be prevented in experimental tests. In the numerical model and similarly to the definition of $E_0$, a microscopic tangential stiffness modulus $E_{ti}$ is defined (in N/m$^3$) by Eq. (7). In the numerical modelling, the value of $E_{ti}$ considered is much smaller than the value of $E_0$.

$$E_{ti} = K_{ti}/S \tag{7}$$

where $S$ represents the influence area of the contact ($S = \pi D^2/4$ for a spherical particle with a diameter $D$).

The geosynthetic sheets are defined by thin triangular elements of thickness $e$ joined together. To guarantee the regularity and the continuity of the contact surface during stretching of the sheet between the triangular elements and the soil particles, cylinders and spheres of diameter $e$ are positioned respectively at the edges and on the nodes of each triangular element (Fig. 4). Thanks to the continuous contact surface, the frictional forces are preserved when a soil element moves from one sheet element to another.

The response induced by the incremental friction law Eq. (4). was tested: a spherical particle in contact with a fixed sheet element was displaced on an elliptical path. A vertical force kept the contact persistent. The aim of this modelling was to verify that the friction effort remained as the soil particle moved from one sheet element to another, but also to appreciate the influence of $E_{ti}$ on the macroscopic friction behaviour induced by the selected

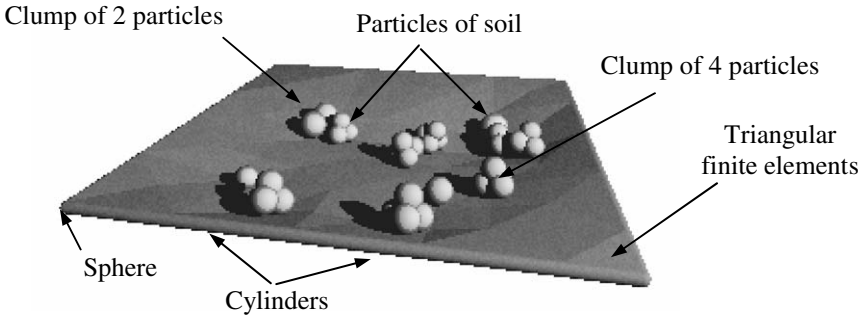


**Fig. 4.** Principle of interaction between finite and discrete elements.

Please cite this article in press as: Villard P et al., Coupling between finite and discrete element methods for the modelling ..., Comput Geotech (2009), doi:10.1016/j.compgeo.2008.11.005

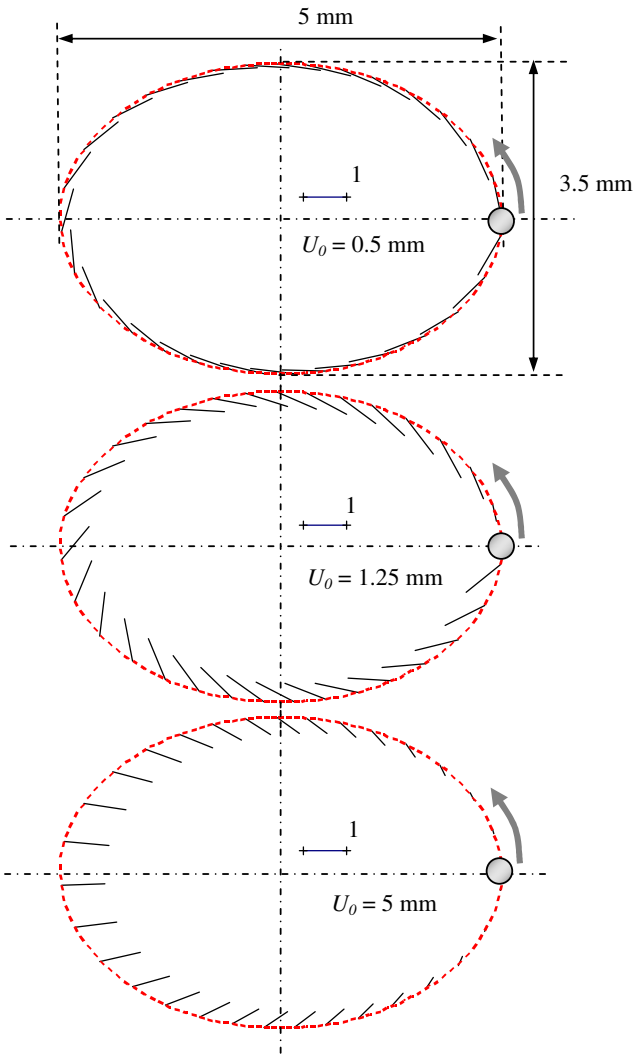


**Fig. 5.** Friction mobilization ratio and orientation of tangential forces for different contact points during the displacement of the soil particle on the sheet elements.

micro-mechanical friction law. Several values of tangential stiffness moduli were tested so that the maximal tangential forces were obtained for relative displacements of 0.5, 1.25 and 5 mm.

Fig. 5 gives the friction mobilization ratio ($\tau/\tau_{max}$) and the orientation of tangential forces at different contact points (solid lines) during the displacement of the soil particle on the sheet elements (dashed line).

We note in Fig. 5 that the greater the tangential stiffness modulus $E_{ti}$, the sooner full mobilization of the friction occurs. For a large value of $E_{ti}$ ($U_0$ = 0.5 mm), the friction forces immediately oppose the displacement of the particle because the relative displacement necessary to obtain a maximal tangential stress $\tau_{max}$ is small compared to the amplitude of the global trajectory of the soil particle. Conversely, as $E_{ti}$ decreases, the friction forces between the soil particle and the sheet element are less and less tangential to the trajectory of the soil particle. For the smallest value of $E_{ti}$ tested ($U_0$ = 5 mm), the frictions no longer oppose the displacement of the particle because the friction threshold is not reached (elastic behaviour).

The behaviour of the sheet elements is governed by a resolution algorithm involving a time step $\Delta t$, similar to the one used for the discrete elements. Thus, the displacement of each finite element is managed by Newton's second law of motion. Basic relations characteristic of the mechanical behaviour of the triangular elements [28,29] are used to obtain the contact forces acting between two jointed finite elements, knowing the stretching and displacement of each node. At each calculation step, the interacting contact forces are deduced from the updated overlaps between the sheet elements and the soil particles. Knowing the contact forces applied to each element (clusters and sheet elements), Newton's second law of motion gives the acceleration, speed and displacements of each element between two steps of successive times. The new relative positions of the elements initiate a new calculation step.

## 3. Comparison between the numerical model, analytical solution and experimental results of a true-scale experiment

### 3.1. The true-scale experiment

The true-scale experiment chosen to validate the numerical model was an instrumented reinforced embankment submitted to artificial subsidence. This experimental case, reported in detail by Briançon et al. [5], is an interesting way to test the numerical model because it involves:

- the behaviour of a granular layer under large displacements inducing shearing and load transfer mechanisms,
- the interaction between a reinforcement geosynthetic and a granular soil,
- the sliding and stretching of the geosynthetic sheet in the anchorage area.

The experimental embankment was 30 m long by 1 m wide in the instrumented cross section (Fig. 6). It consisted of a granular layer of a thickness of 0.5 m resting on a geosynthetic sheet reinforced in the longitudinal direction. A 2 m long and 1 m wide cavity, filled with two balloons, was first implanted in the subsoil under the geosynthetic sheet, 2 m from one end of the embankment. The progressive emptying of the balloons then made it possible to reproduce the subsidence mechanism.

Various laboratory tests were carried out in order to validate the use of a new technology for strain measurement and to obtain

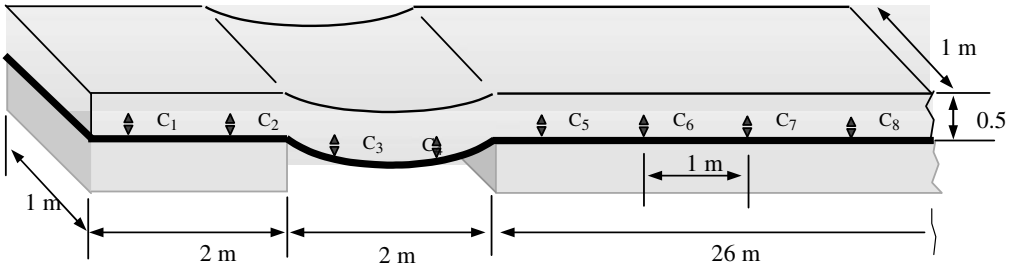


**Fig. 6.** Geometry of the reinforced embankment submitted to localised sinkhole.

Please cite this article in press as: Villard P et al., Coupling between finite and discrete element methods for the modelling ..., Comput Geotech (2009), doi:10.1016/j.compgeo.2008.11.005

the geometrical and physical parameters of the materials used: product test, strain tests, damage tests in a shear box and membrane effect tests [4]. These tests allowed the main parameters of soil, geosynthetic and interfaces to be determined.

The geosynthetic used was a non-woven needle punched geotextile reinforced by polyester yarns in the main production direction. The stiffness of the geosynthetic in the reinforced direction was $J = 1100$ kN/m and the tensile force at break $T_{max}$ (obtained for 12% strain) was 125 kN/m. The secant stiffness obtained in the transverse direction was 25 kN/m.

The granular layer was made of coarse elements of diameters ranging from 0.02 to 0.04 m (granular material – called ballast – commonly used for building the underlying fill of French railway embankments [1,25]). The unit weight of the granular material $\gamma$ was 17 kN/m$^3$ and the internal friction angle $\varphi$ obtained under weak confinement 44°. The friction laws at the soil/geosynthetic interface were assumed to be the Coulomb friction laws (Fig. 3). The interface friction angles [5]; Briançon et al., 2006; [31], obtained by shearing tests, were respectively, $\delta_{upper} = 30°$ between granular soil and geotextile sheet and $\delta_{lower} = 25°$ between the subsoil and geosynthetic.

The strains in the geosynthetic reinforcement were measured continuously during the experiment (Fig. 6) at many points (1 m spacing) by Bragg Gratings sensors [4] incorporated in optical fibres [27] fixed on the geosynthetic sheet (Geodetect System). Manual measurements were taken during the experiment to obtain the surface settlements and vertical displacements of the sheet above the cavity.

Five months after removing the balloons, new measurements were performed. Small increases in geosynthetic strains were noticed above the cavity and in the anchorage areas, resulting from the progressive transfer of load at the interface and in the granular layer.

### 3.2. The analytical design method

Several analytical methods [18,8]; German rules [15,2,29,3,30] based on experimental and theoretical researches [23,22,17,20] are usually proposed to describe the behaviour of reinforced embankments submitted to localized sinkholes. Recent developments [6,7] allow vertical and horizontal displacements of the geosynthetic sheet to be predicted, knowing the stiffness of the geosynthetic ($J$), the interface friction parameters ($\delta_{upper}$ and $\delta_{lower}$), the soil parameters ($\varphi$ and $\gamma$), the height of the embankment ($H$) and the size of the cavity ($L$). The interest of this method compared to the others lies in the fact that it takes into account the stretching of the geosynthetic in anchorage areas and the increase in stress at the edges of the cavity, in addition to the usual mechanisms (membrane effect). The major assumptions used to formulate the analytical design method are:

- The problem is plane-strain.
- The subsoil under the geosynthetic is assumed to be non deformable.
- The loads $q$ and $q_0$ acting on the geosynthetic sheet above the cavity and in the anchorage areas (Fig. 7) are vertical and uniformly distributed. Load $q$ is calculated by the limit equilibrium method developed by Terzaghi [26].
- The geosynthetic sheet is reinforced in one direction (monodirectional reinforcement). Its behaviour is assumed to be linear elastic: $T = J * \varepsilon$ where $T$ and $J$ *are, respectively,* the tensile force and the stiffness of the geosynthetic defined per unit width and $\varepsilon$ the sheet strain.
- The geosynthetic over the cavity takes a membrane shape due to the vertical loads $q$ applied [16,18,19].
- There is a decrease in tensile force in the geosynthetic at the edge of the cavity due to the change of orientation of the sheet.
- The horizontal displacements of the sheet in the anchorage areas result from the stretching and the sliding of the geosynthetic sheet.
- The friction laws at the soil/geosynthetic interfaces are the Coulomb friction laws defined in Fig. 3: $\sigma_n = q_0$ in the anchorage area and $\sigma_n = q$ above the cavity.
- There is an increase in the volume of soil over the cavity during collapse that leads to reduce the surface settlement. The ratio between the new soil volume and the initial soil volume is called the expansion coefficient Ce.
- The boundary conditions allow finite or infinite geosynthetic lengths on the right and on the left of the cavity (LGl and LGr) to be taken into account.

### 3.3. The numerical simulation

Due to the longitudinal symmetry, the numerical model was 10 m long by 0.5 m in width. In order to reproduce the experimental characteristics (cf. part 3.1) of the soil embankment the granular material was modelled with 10,000 clusters (diameters ranging from 0.02 to 0.04 m) made of two imbricated particles (as defined in Section 2.2) and positioned in space with a random distribution at porosity $\eta = 0.342$. The geometry of the numerical assembly of particles was therefore rather close (size grains and density) to that in the experiment carried out.

Horizontal and vertical rigid walls were used to define the boundary conditions. The macro mechanical behaviour of the

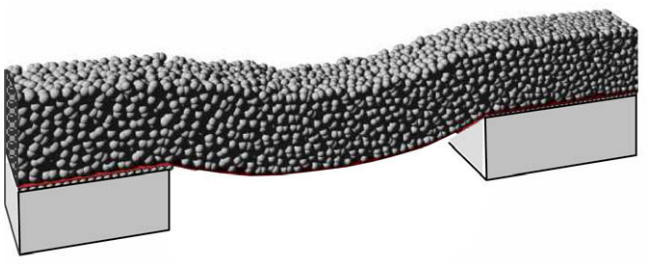

**Fig. 8.** View of the numerical modelling of the embankment after the skinhole.

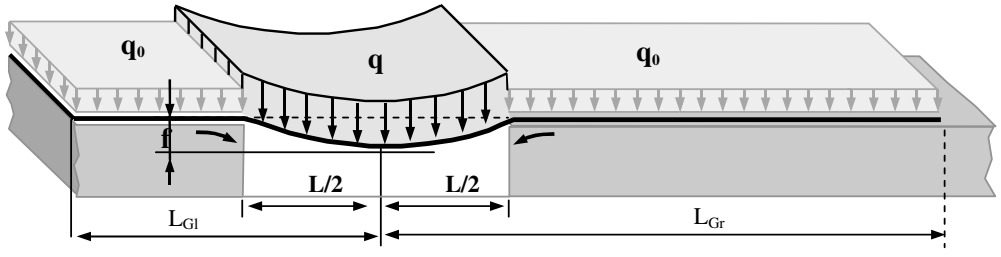


**Fig. 7.** Geometry of the reinforced embankment used in the analytical design method.

assembly of particles was that given in Fig. 1. For an initial porosity of 0.342, the macroscopic peak friction angle of the granular material was 44°. The apparent density of the granular soil was 17 kN/m$^3$.

The rigid subsoil was modelled by a set of spherical particles of 0.04 m diameter for which only vertical displacement was allowed, and no rolling admitted. The vertical displacement of the subsoil particles was governed by elastic behaviour equivalent to that of a solid with an elastic modulus of 250 MPa and a height of 0.5 m.

The geosynthetic sheet was modelled with 1360 triangular finite elements of thickness 0.005 m. The 2 m-long left part of the sheet was free, unlike the 6 m-long right part which was fixed at its extremity. The non-woven needle punched support was modelled by a set of eight orientations of fibres uniformly distributed in a plan with an equivalent tensile rigidity of 25 kN/m. The polyester yarns were modelled by specific fibres oriented in the longitudinal direction with an equivalent tensile rigidity of 1100 kN/m.

The friction angle between the geosynthetic sheet and the granular soil was 30°, while that between the subsoil and the geosynthetic sheet was 25°. The normal contact rigidity between soil and the geosynthetic sheet ensured that there was no interpenetration between the elements. The microscopic tangential stiffness modulus between finite and discrete elements was $E_{ti}$ = 10 MN/m$^3$ ($U_0$ was around 0.5 mm for the normal stress acting at the interface).

At both sides of the cavity, the lateral boundary conditions were imposed using frictional rigid walls (friction angle of 44°).

The numerical sample was first equilibrated under gravity using a horizontal plate over the cavity to prevent any vertical displacements. The activation of the subsidence mechanisms was obtained by removing the horizontal plate. The mechanisms studied were the stretching and sliding of the geosynthetic sheet in the anchorage areas, movement of the particles of the soil embankment and vertical displacements of the geosynthetic sheet over the cavity (Fig. 8).

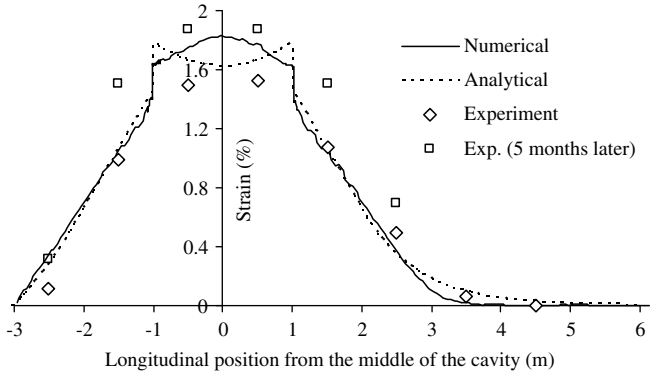


**Fig. 9.** Comparison between numerical, analytical and experimental strains.

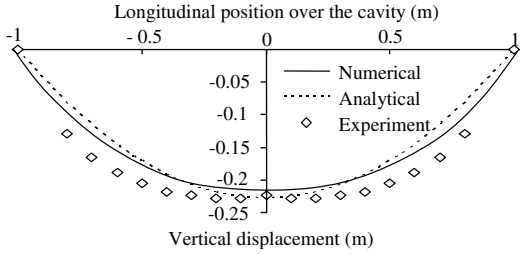


**Fig. 10.** Comparison between numerical, analytical and experimental vertical displacements of the geosynthetic sheet.

### 3.4. Comparison between the analytical, experimental and numerical models

The comparison between the numerical model, analytical design method and experimental results is based on the measurement of the vertical displacements of the geosynthetic sheet and on the experimental values of the strain gauges just after emptying the balloons and 5 months later (Figs. 9 and 10). The parameters used for the analytical design method were: $L$ = 2 m, $H$ = 0.5 m, $\gamma$ = 17 kN/m$^3$, $\varphi$ = 44°, $C_e$ = 1.05, $q_0 = \gamma H$ = 8.5 kN/m$^2$, $J$ = 1100 kN/m, $\delta_{upper}$ = 30°, $\delta_{lower}$ = 25°, $U_0$ = 5 mm, $L_{Gl}$ = 3 m and $L_{Gr} = \infty$.

The comparison between numerical, analytical and experimental results shows that the numerical model reproduces the main mechanisms involved during the subsidence of the reinforced embankment in a satisfactory manner: membrane effect, stretching, friction, and sliding of the geosynthetic sheet in the anchorage areas, increase in strain (and tensile force) at the edges of the cav-

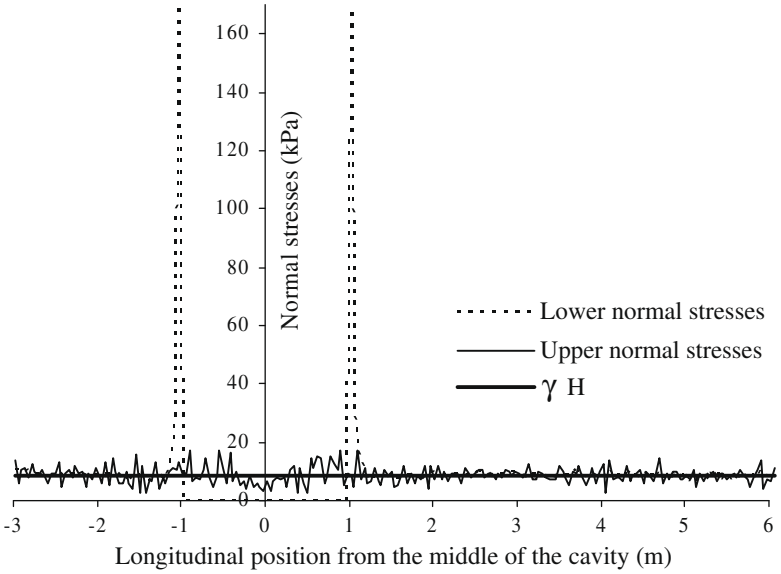


**Fig. 11.** Distribution of the normal stresses on the upper and lower sides of the geosynthetic.

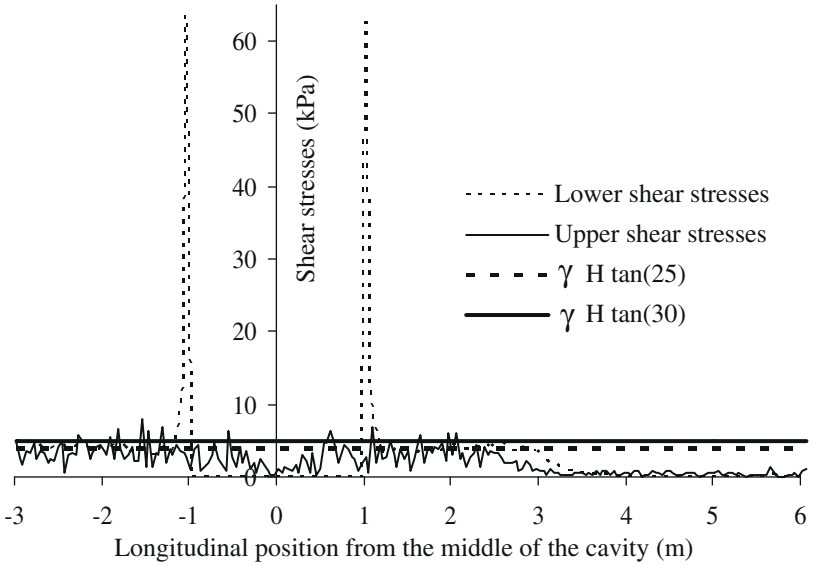


**Fig. 12.** Distribution of the shear stresses on the upper and lower sides of the geosynthetic.

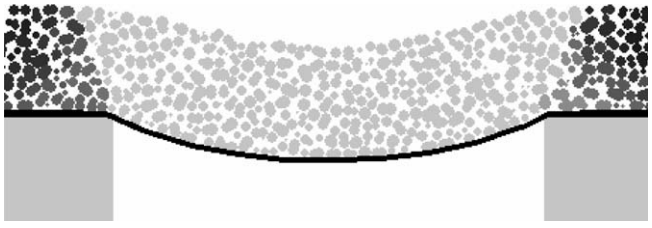

**Fig. 13.** Displacement of the granular soil particles.

ity and the behaviour of the granular soil layer under large displacements.

The small differences obtained between analytical and numerical results are due to the simplifying assumptions used to develop the analytical design method: the vertical loads are uniformly applied on the geosynthetic sheet, there is no deformation of the subsoil, no friction between granular soil and the part of the geosynthetic sheet located over the cavity, no rolling and no horizontal displacements of the granular particles during the stretching of the sheet in the anchorage areas. The most important difference between the design method and the numerical method is due to differences in the frictional shear stresses between soil and geosynthetic over the cavity.

In order to highlight the behaviour of the granular soil layer and its interaction with the geosynthetic sheet, additional numerical results are presented in Figs. 10–14. Fig. 11 shows the distribution of normal stresses acting on the upper and lower sides of the geosynthetic sheet. On the lower side of the sheet, we can notice an increase in vertical stress at the edges of the cavity due to the transfer of the load (weight of the soil embankment located over the cavity) to the subsoil by membrane effect. On the upper side we can notice, by comparison with the value of the vertical stresses due to the weight of the soil embankment ($\gamma H$), that there is no significant arching effect in the present case (low value of the ratio $H/L = 0.25$). The assumption used for the analytical design method of uniform vertical load acting on the geosynthetic is satisfactory enough for granular material and for the geometry studied here.

Fig. 12 shows distribution of the shear stresses acting on the upper and lower interfaces of the geosynthetic sheet. As mentioned before, we can notice an increase in shear stresses at the edges of the cavity due to local phenomena. The comparison with the values of the maximal shear stresses that can be obtained at

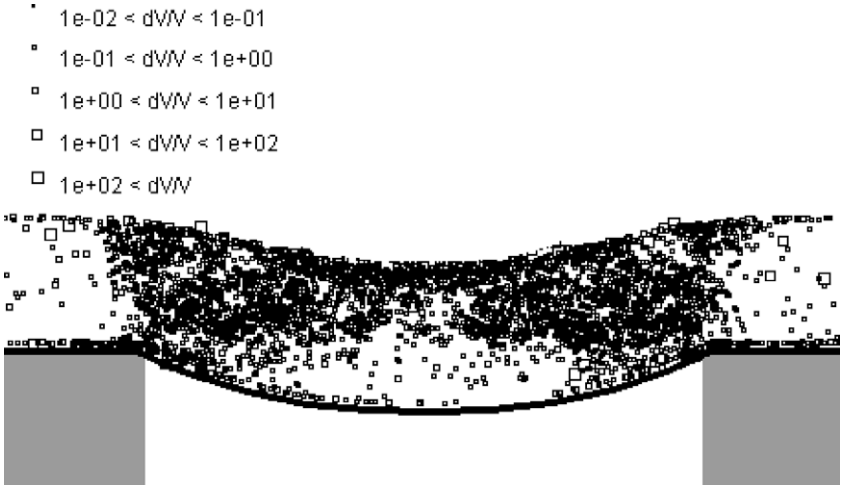


**Fig. 14.** Distribution and intensities of the first invariant $dV/V$ of the strain tensor.

each interface ($\gamma H \tan \delta_{lower}$ and $\gamma H \tan \delta_{lower}$) shows that friction is partially mobilized on the right side of the cavity, and fully completed on the left side. Over the cavity, friction between soil particles and geosynthetic induces additional shear stresses and leads to an increase in the strain over the cavity. Note that the fluctuation of the curves presented in Figs. 10 and 11 results from the discrete modelling of the soil embankment.

The displacements of the soil particles in a vertical cross section of the cavity are given in Fig. 13. We can see that the area of soil implicated in the subsidence is located over the cavity. The stretching of the sheet in the anchorage areas induces horizontal movement of the soil particles in the vicinity of the geosynthetic sheet. Based on a method first presented by Cundall and Strack [12] and applied in 2D by Calvetti et al. [9], a strain tensor was calculated for each tetrahedron of the Delaunay tessellation of the particle assembly. The first invariant – referred to as $dV/V$ – of this strain tensor was deduced and represented in Fig. 14. The amplitudes of the value of the first invariant reflect the intensity of volumetric strains in the granular layer. Except in the central part of the cavity in the lower part of the layer (near the geotextile) where the particle assembly is not disordered, soil expansion is considerable. The ratio between the initial and final volumes of the part of the granular embankment located over the cavity gives an expansion coefficient of the modelled granular soil of about 1.09.

## 4. Conclusion

The numerical model developed here and coupling finite element and discrete element methods allows the behaviour of an embankment reinforced by geosynthetic sheets to be reproduced in a satisfactory manner. The discrete model is well adapted to take account of realistic phenomena involved in the granular soil layer: shearing, expansion, load transfer and large displacements (subsidence and collapse). The finite element model makes it possible to describe the fibrous structure of the geosynthetic sheet, its mechanical behaviour (stretching and membrane effect) and its interaction with the soil (friction and sliding).

For the current plane-strain application involving a thin layer of granular material, the numerical results provide a good match with the analytical results. In more sophisticated cases, due to the simplifying assumptions made to develop the analytical design method, it could be possible to have large differences between analytical and numerical results. This is probably the case for three-dimensional applications (cylindrical or non symmetrical cavities), for greater embankment thickness values (load transfer mechanisms in soil embankments are sophisticated), for cohesive soil (the collapse mechanisms for cohesive soil are rather different from these observed for granular material) and for geosynthetic sheets reinforced in several directions.

One of the major interests of the numerical model is its ability to take account of a wide range of soil behaviour, embankment heights and cavity shapes. Parametric studies could be performed easily in order to investigate the influence of the main parameters and to improve the usual design methods. For instance, the analytical design of cohesive soil embankments subjected to localised sinkhole remains problematic due to the lack of the experimental results necessary to validate the numerical models.

## References

[1] AFNOR, 2003. Granulats pour ballast de voies ferrées. French Standard NF EN-13450, 30p.
[2] Blivet JC, Khay M, Villard P., Gourc JP. Design method for geosynthetic as reinforcement for embankment subjected to localized sinkholes. In: GeoEng2000, international conference on geotechnical and geological engineering, Melbourne, Austria; 2000. p. 1–6.
[3] Blivet JC, Khay M, Gourc JP, Giraud, H. Design considerations of geosynthetic for reinforced embankments subjected to localized subsidence. In: Proceedings of the geosynthetics' 2001 Conference, February 12–14, 2001, Portland, Oregon, USA; 2001. p. 741–54.
[4] Briançon L, Nancey A, Caquel F, Villard P. New technology for strain measurements in soil and the survey of reinforced earth constructions. In: Proc. of EUROGEO 3, Munich, Germany, vol. 2 2004. p. 471–6.
[5] Briançon L, Nancey A, Villard P. Development of Geodetect: a new warning system for the survey of reinforced earth constructions. Stud Geotech Mecha 2005;1–2:23–32.
[6] Briançon L, Villard P. Dimensionnement des renforcements géosynthétiques de plates-formes sur cavités. Revue Française de Géotechnique 2006;117: 51–62.
[7] Briançon L, Villard P. Design of geosynthetic reinforcements of platforms subjected to localised sinkholes. Geotext Geomembr 2008;26(5):416–28.
[8] British Standard BS 8006. Code of practice for strengthened/reinforced soils and other fills. British Standard Institution, London; 1995. 162p.
[9] Calvetti F, Combe G, Lanier J. Experimental micromechanical analysis of a 2D granular material: relation between structure evolution and loading path. Mech Cohes-Frict Mater 1997;2:121–63.
[10] Chareyre B, Villard P. Dynamic spar elements and DEM in two dimensions for the modelling of soil-inclusion problems. J Eng Mech – ASCE 2005;131(7): 689–98.
[11] Cundall PA, Strack ODL. A discrete numerical model for granular assemblies. Geotechnique 1979;29(1):47–65.
[12] Cundall PA, Drescher A, Strack ODL. Numerical experiments on granular assemblies: measurements and observations. In: IUTAM conference on deformation and failure of granular materials, Delft; 1982.
[13] Donzé FV, Magnier SA. Formulation of a three-dimensional numerical model of brittle behaviour. Geophys J Int 1995;122:790–802.
[14] Donzé FV, Magnier SA. Spherical discrete element code. In: Discrete element project – GEOTOP, Université du Québec, Montréal, Report No. 2; 1997.
[15] EBGEO: Empfehlungen für Bewehrungen aus Geokunststoffen. Deutesche Gesellschaft für Geotechnik (Hrsg). Verlag Ernst Sohn, Berlin; 1997.
[16] Espinoza RD. Soil-geotextile interaction: evaluation of membrane support. Geotext Geomembr 1994;13:281–93.
[17] Giraud H. Renforcements des zones d'effondrement localisé - Modélisations physique et numérique. PhD thesis, University of Grenoble, France; 1997.
[18] Giroud JP, Bonaparte R, Beech JF, Gross BA. Design of soil layer-geosynthetic systems overlying voids. Geotext Geomembranes 1990;9:11–50.
[19] Giroud JP. Determination of geosynthetic strain due to deflexion. Geosynth Int 1995;2:635–41.
[20] Gourc JP, Villard P, Giraud H, Blivet JC, Khay M, Imbert B, et al. Sinkholes beneath a reinforced earthfill – a large scale motorway and railway experiment. In: Proceedings of Geosynthetics' 99, Boston, vol. 2, Massachusetts, USA, 28–30 April 1999. p. 833–46.
[21] Gourc JP, Villard P. Reinforcement by membrane effect: application to embankments on soil liable to subsidence. In: Proceedings of the 2nd Asian Geosynthetics Conference, vol. 1, ASIA 2000, Kuala Lumpur, Malaysia, 29–31 May 2000. p. 55–72.
[22] Kempton GT, Lawson CR, Jones CJFP, Demerdash M. The use of geosynthetics to prevent the structural collapse of fills over areas prone to subsidence. In: Proceedings of EUROGEO 1, Maastricht, Netherlands, 30 September–2 October 1996. p. 317–24.
[23] Kinney TC, Connor B. Geosynthetics supporting embankments over voids. J Cold Reg Eng 1987;1:158–70.
[24] Salot C. Modélisation du comportement mécanique d'un matériau granulaire composite par la Méthode des Eléments Discrets, Université Grenoble 1, PhD thesis; 2007. 236p.
[25] Saussine G. Contribution à la modélisation de granulats tridimensionnels: application au ballast. Université de Montpellier II, PhD thesis; 2004. p. 22, [chapter 1.1.3].
[26] Terzaghi K. Theoretical soil mechanics. New York: John Wiley & Sons; 1943.
[27] Udd E. In: Udd E, editor. Fiber optic smart structures in fiber optic sensors: an introduction for engineers and scientists. Wiley; 1991.
[28] Villard P, Giraud H. Three-dimensional modelling of the behaviour of geotextile sheets as membrane. Text Res J 1998;68:797–806.
[29] Villard P, Gourc JP, Giraud H. A geosynthetic reinforcement solution to prevent the formation of localized sinkholes. Can Geotech J 2000;37:987–99.
[30] Villard P, Gourc JP, et Blivet JC. Prévention des risques d'effondrement de surface liés à la présence de cavités souterraines: une solution de renforcement par géosynthétique des remblais routiers et ferroviaires. Rev Franç Géotechn 2002;99:23–34.
[31] Villard P, Briancon L. Design of geosynthetic reinforcements of platforms subjected to localized sinkholes. Can Geotech J 2008;45(2):196–209.

Please cite this article in press as: Villard P et al., Coupling between finite and discrete element methods for the modelling ..., Comput Geotech (2009), doi:10.1016/j.compgeo.2008.11.005